Atrazine Chlorohydrolase from *Pseudomonas* Sp. Strain ADP Is a Metalloenzyme†

Jennifer L. Seffernick,‡,§ Hugh McTavish,‡,|| Jeffrey P. Osborne,‡,§ Mervyn L. de Souza,‡,§,⊥ Michael J. Sadowsky,▽,§,○ and Lawrence P. Wackett*,‡,▽,§

Department of Biochemistry, Molecular Biology, and Biophysics, Biotechnology Institute, Center for Microbial and Plant Genomics, and Department of Soil, Water, and Climate, University of Minnesota, St. Paul, Minnesota 55108

Received June 13, 2002; Revised Manuscript Received September 18, 2002

ABSTRACT: Atrazine chlorohydrolase (AtzA) from *Pseudomonas* sp. ADP initiates the metabolism of the herbicide atrazine by catalyzing a hydrolytic dechlorination reaction to produce hydroxyatrazine. Sequence analysis revealed AtzA to be homologous to metalloenzymes within the amidohydrolase protein superfamily. AtzA activity was experimentally shown to depend on an enzyme-bound, divalent transition-metal ion. Loss of activity obtained by incubating AtzA with the chelator 1,10-phenanthroline or oxalic acid was reversible upon addition of Fe(II), Mn(II), or Co(II) salts. Experimental evidence suggests a 1:1 metal to subunit stoichiometry, with the native metal being Fe(II). Our data show that the inhibitory effects of metals such as Zn(II) and Cu(II) are not the result of displacing the active site metal. Taken together, these data indicate that AtzA is a functional metalloenzyme, making this the first report, to our knowledge, of a metal-dependent dechlorinating enzyme that proceeds via a hydrolytic mechanism.

Chlorinated compounds have been heavily used throughout industry and agriculture. These compounds often contaminate soils and persist until they are metabolized by microorganisms (*1*−*8*). Commercial chlorinated compounds designed for environmental release include insecticides, fungicides, and herbicides. Atrazine (2-chloro-4-ethylamino-6-isopropylamino-*s*-triazine) and simazine (2-chloro-4-ethylamino-6-ethylamino-*s*-triazine) are widely used members of a very successful class of chlorinated herbicides that contain an *s*-triazine ring.

Bacteria that use atrazine or simazine as their sole nitrogen source for growth have been identified (*9*−*11*). *Pseudomonas* sp. ADP is one of the most well-studied atrazine-degrading bacteria and metabolizes atrazine to carbon dioxide, ammonia, and chloride ion (*12*). The catabolic pathway is initiated by three enzymes, AtzA, AtzB, and AtzC,[1] which catalyze hydrolytic reactions that transform atrazine via hydroxyatrazine and *N*-isopropylammelide to cyanuric acid (Scheme 1).

Scheme 1: Upper Part of the Catabolic Pathway for the Degradation of Atrazine via AtzA, AtzB, and AtzC

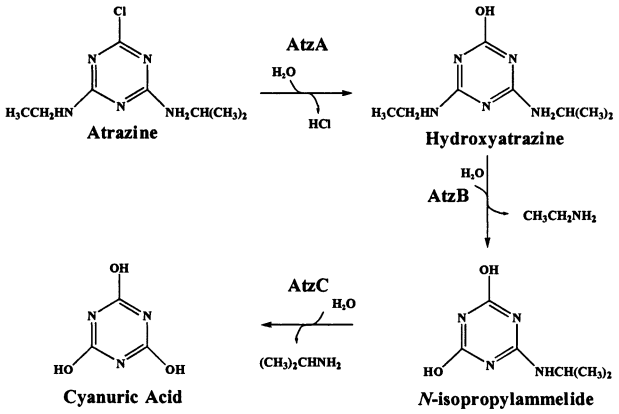

Atrazine chlorohydrolase, AtzA, has been purified to homogeneity from recombinant *E. coli* and shown to incorporate ^{18}O from water into the hydroxyatrazine product (*13*). AtzA has a predicted subunit molecular weight of 52421, as derived from the gene sequence, and was shown by gel filtration to have a holoenzyme molecular weight of 245000 (*13*). Thus, AtzA most likely has either an α_4 or α_5 subunit structure. Initial analysis of the metal content of AtzA revealed substoichiometric quantities of transition metals (*13*). This result was consistent with reports of other bacterial hydrolytic dehalogenases, none of which are known to be metalloenzymes. For example, high-resolution crystal structures for haloalkane dehalogenase (*14*), 4-chlorobenzoyl CoA dehalogenase (*15*), and L-2-haloacid dehalogenase (*16*) indicate that none of these enzymes contain a metal. Instead, they use an active site aspartate as a nucleophile to displace the halide anion and form a covalent enzyme intermediate, which is subsequently hydrolyzed by water (*14*−*16*).

† Financial support was provided by Syngenta Crop Protection and by NIH Training Grant GM08347.

* To whom correspondence should be addressed at the Department of Biochemistry, Molecular Biology, and Biophysics, 1479 Gortner Ave.; University of Minnesota, St. Paul, MN 55108. Phone: (612) 625-3785. Fax: (612) 625-1700. E-mail: wackett@biosci.cbs.umn.edu.

‡ Department of Biochemistry, Molecular Biology, and Biophysics.

§ Center for Microbial and Plant Genomics.

|| Current address: Schwegman, Lundberg, Woessner & Kluth, 1600 TCF Tower; 121 S. 8th St., Minneapolis, MN 55402.

⊥ Current address: Cargill, Inc., P.O. Box 5702, Minneapolis, MN 55440-5702.

▽ Biotechnology Institute.

○ Department of Soil, Water, and Climate.

[1] Abbreviations: AtzA, atrazine chlorohydrolase; AtzB, hydroxyatrazine ethylaminohydrolase; AtzC, *N*-isopropylammelide *N*-isopropylaminohydrolase; TrzA, *s*-triazine hydrolase; DTT, dithiothreitol; ICP-AES, inductively coupled atomic plasma emission spectroscopy; apoAtzA, apoenzyme of AtzA; Co(II)−AtzA, Co(II)-reconstituted apoAtzA; EPR, electron paramagnetic resonance spectroscopy.

10.1021/bi020415s CCC: $22.00
Published on Web 11/01/2002

Initial studies showed that AtzA had very low amino acid sequence identity (<25%) in pairwise comparisons with sequences in the GenBank database. More recently, however, AtzA was discovered to contain consensus amino acid sequences characteristic of proteins in the amidohydrolase protein superfamily described by Holm and Sander (*17*, *18*). It is well-established that many members of the amidohydrolase protein superfamily bind catalytically essential transition metals: urease contains Ni(II), adenosine deaminase contains Zn(II), and cytosine deaminase from *E. coli* has Fe(II) (*19*−*21*). Therefore, more detailed studies concerning the influence of metals on AtzA activity and the metal content of AtzA were required.

In this study, we report that AtzA is a metalloenzyme that uses Fe(II), Mn(II), or Co(II) to catalyze the hydrolytic dechlorination of atrazine. Spectroscopic analyses indicated that the Co(II) enzyme is likely a five-coordinate species. To our knowledge, AtzA is the first reported metal-dependent chlorohydrolase.

MATERIALS AND METHODS

Bacterial Strains and Protein Purification. Atrazine chlorohydrolase (AtzA) was purified from *Escherichia coli* DH5α (pMD4), containing the cloned *atzA* gene (*22*). Cultures were grown overnight at 37 °C in Luria−Bertani (LB) medium (*23*), supplemented with chloramphenicol (30 μg/mL). Cells were lysed and protein purified as previously described (*13*).

Enzyme Assay. Atrazine hydrolysis was assayed spectrophotometrically at 262 nm in 25 mM 3-(*N*-morpholino)-propanesulfonic acid (MOPS) buffer, pH 6.9, 10 mM KCl (buffer A) with 150 μM atrazine at 23 °C as previously described (*24*). The extinction coefficient of atrazine in this buffer was determined to be 3.42 mM^{-1} cm^{-1}. The water solubility of atrazine, 153 μM at 22 °C, is very close to the estimated K_m for AtzA of 149 μM (*13*, MSDS Novartis), making measurement of accurate kinetic parameters difficult. Reproducible specific activity measurements were observed with single-enzyme preparations and are reported here.

Protein Concentration Determinations. Protein concentrations for quantitative metal analysis studies were determined using a Beckman 6300 amino acid analyzer (Beckmen Coulter, Fullerton, CA) at the Microchemical Facility, Human Genetics Institute, University of Minnesota. Routine determinations of protein concentrations were performed with the BioRad Protein Reagent (Hercules, CA), using bovine serum albumin as a standard.

Influence of Metals on Native, Isolated AtzA. Enzyme was incubated with a 0.2 mM concentration of various metal salts for 30 min at 23 °C. Specific activities were determined in buffer A, as described above, with final metal concentrations of 0.1 mM. Among the compounds tested were $CoCl_2$, $MnSO_4$, $NiCl_2$, $CuCl_2$, $ZnSO_4$, $FeCl_3$, and $FeSO_4$. To ensure that Fe(II) remained in the reduced state, 0.5 mM cysteine and 1.5 mM dithiothrietol (DTT) were added to incubation and reaction buffers containing $FeSO_4$. The following metal salts were also tested at the concentrations indicated: 1 mM $CaCl_2$, 2 mM $MgCl_2$, 1 M KCl, 1M NaCl, 1 M Na_2SO_4, and 1 M K_2SO_4.

Metal Analysis. AtzA was hydrolyzed and the metal content was quantified via inductively coupled plasma atomic emission spectroscopy (ICP-AES) as previously described (*13*).

Apoenzyme Preparation. Apoenzyme (apoAtzA) was prepared by incubating 57 μM purified AtzA in 25 mM MOPS (pH 6.9), containing 10 mM KCl and 1 mM 1,10-phenanthroline (buffer B) at 30 °C for 90 min. The solution was concentrated using a Centriprep 10 filtration unit (Amicon, Beverly, MA) and loaded onto a 1.5 × 13 cm Sephadex G-25 column equilibrated with buffer A to separate the protein from metal-bound 1,10-phenanthroline.

Influence of Metals on Apoenzyme. ApoAtzA (33 μM) was incubated with buffer A containing a 0.2 mM concentration of various metal salts for 30 min at 23 °C and assayed as described above. Concentrations of 0.5 mM $CaCl_2$ and 1 mM $MgCl_2$ were also used.

Reconstitution of Apoenzyme with Metals. ApoAtzA was incubated with 0.5 mM metal, in the presence or absence of 100 mM sodium bicarbonate, for 15 min to 12 h at 23 °C. The reconstituted enzyme was passed through a Sephadex G-25 column and eluted with buffer A to remove unbound metals.

Ultraviolet−Visible Spectroscopy. Two samples of Co(II)-reconstituted apoAtzA (Co(II)−AtzA), at 267 and 438 μM, respectively, were prepared from different native enzyme batches by placing apoenzyme in an anaerobic cuvette that was sealed with a rubber septum and made anaerobic by flushing with moist argon gas. An anaerobic Co(II) stock solution, prepared by mixing $CoCl_2$ crystals with buffer in an argon atmosphere, was added to the apoenzyme under anaerobic conditions at a 0.9 metal to subunit stoichiometry. Spectra from 200 to 1100 nm were taken in the presence and absence of the substrate analogue aminoatrazine. Extinction coefficients were determined on the basis of Co(II) concentrations, using a baseline zero absorbance at 970 nm. Data were acquired using a Beckman DU 640 spectrophotometer (Beckman Coulter). Control samples in 25 mM MOPS buffer (pH 6.9) were also analyzed and included buffer alone, apoenzyme, $CoCl_2$, $FeSO_4$, $FeCl_3$, aminoatrazine, or $CoCl_2$ in the presence of aminoatrazine.

Electron Paramagnetic Resonance (EPR) Spectroscopy. Samples used for UV−vis spectroscopy were transferred under an argon atmosphere to quartz EPR tubes and frozen by slow immersion in liquid nitrogen. X-band EPR spectroscopy was performed using a Bruker E500 spectrometer (Billerica, MA) equipped with an Oxford Instruments ESR-10 liquid helium cryostat. EPR spectra were manipulated with WinEPR 2.11 (Bruker) and simulated following a protocol for the high-spin $S = {}^3/_2$ Co(II) spectra (*25*, *26*). The g_{eff} values were estimated using simulations from the WinEPR Simfonia 1.25 program (Bruker) that treated the $S = {}^3/_2$ high-spin Co(II) species as an effective $S = {}^1/_2$ system. The program Rhombo, courtesy of Professor W. R. Hagen (Delft University of Technology, The Netherlands), was subsequently used to determine the nearest theoretically allowed g_{eff} values from isotropic **g** tensor and rhombicity (E/D) values. The correspondence between the simulated and theoretical g_{eff} values indicated the quality of the simulation. Values for $g_{eff(x,y,z)}$ from simulation are presented, followed by those from theory in parentheses.

Power saturation studies were used to estimate the coordination number of the metal center (*27*−*29*). $P_{1/2}$ values for Co(II)−AtzA were determined at six temperatures ranging from 7.9 to 12 K. The program ORIGIN 5.0 (OriginLab Corp., Northampton, MA) was used to iteratively

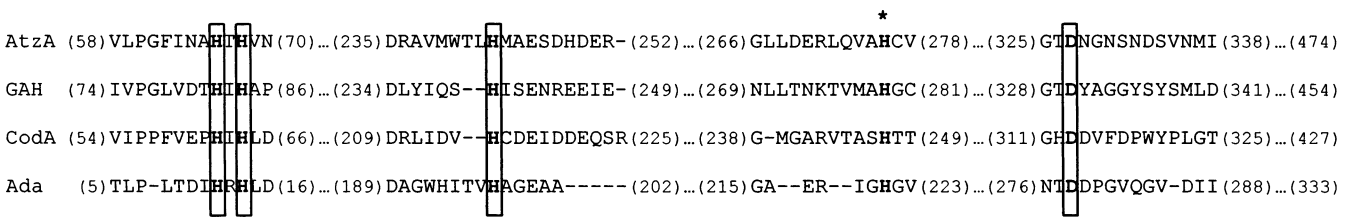

FIGURE 1: Sequence alignment of AtzA with other members of the amidohydrolase superfamily. AtzA is from *Pseudomonas* ADP (g6226558), guanine deaminase (GAH) from *Mus musculus* (g9910725), cytosine deaminase (CodA) from *E. coli* (g116845), and adenosine deaminase (Ada) from *E. coli* (g7428273). Boxed residues are metal ligands established by X-ray crystallography for Ada and CodA, and corresponding residues in the other proteins. The conserved histidine shown in the Ada and CodA crystal structures to hydrogen bond to the nucleophilic water is indicated (*).

Table 1: Influence of Metal Salts on the Activity of Native AtzA[a]

addition	% relative native activity	addition	% relative native activity
none	100	0.2 mM $CuCl_2$	<0.2
0.2 mM $MnSO_4$	113 ± 4	0.2 mM $ZnSO_4$	<0.2
2 mM $MgCl_2$	109 ± 7	0.2 mM $CoCl_2$	184 ± 13
1 mM $CaCl_2$	94 ± 1	0.2 mM $FeSO_4$, 0.5 mM cysteine, 1.5 mM DTT	168 ± 40
0.2 mM $FeCl_3$	37 ± 23	0.5 mM cysteine, 1.5 mM DTT	22
0.2 mM $NiCl_2$	42 ± 15		

[a] Activities were determined for two different enzyme preparations and expressed as a percentage of the native enzyme activity (4.4 and 3.0 (μmol/min)/mg). Averages of the two preparations are displayed in the table.

fit the plots of power versus the normalized $\log(I/P^{0.5})$ with the equation

$$\log(I/P^{0.5}) = (1 + P/P_{1/2})^{(-b/2)}$$

where I is the peak to peak signal intensity, P is the power, and b is the inhomogeneity parameter with a value ranging from 1 to 3 (*30*).

RESULTS

Sequence Analysis. The amino acid sequence of AtzA was aligned with those of adenosine deaminase and cytosine deaminase. The regions shown in Figure 1 include the four metal ligand residues in adenosine deaminase and cytosine deaminase that have been identified by X-ray crystallography (*20*, *21*). A fifth ligand, water, completes the coordination sphere for adenosine deaminase and cytosine deaminase. Although sequence identities in pairwise comparisons were modest (20−30%), the adenosine deaminase metal ligands are conserved throughout the set, suggesting a functional role for these conserved three histidines and one aspartate in AtzA.

Effect of Metal Ions on Native AtzA Activity. Incubation of native AtzA with various divalent metal cations significantly affected enzyme activity (Table 1). Co(II) and Fe(II) salts increased the activity of freshly isolated enzyme up to 2-fold. Mg(II) and Ca(II) salts had virtually no effect on activity. Cu(II) and Zn(II) salts caused complete inhibition, while Ni(II) and Fe(III) each showed approximately 50% inhibition. Cysteine and DTT were included with Fe(II) to maintain the iron atom in the reduced state, but the reductants alone were not responsible for the activation and, in fact, caused inhibition in the absence of Fe(II). Using a separate enzyme preparation that contained a 1:1 Fe(II) to subunit stoichiometry, the effects of DTT alone were investigated. Addition of Fe(II) by itself resulted in no increase, 99 ± 7%, of native activity, while addition of DTT in the presence or absence of Fe(II) resulted in 86 ± 6% and 86 ± 4% of native activity, respectively.

Quantitation of Bound Metal. The metal content of several enzyme preparations was analyzed by ICP-AES (Table 2). The native enzyme, as isolated from the AtzA-overproducing strain of *E. coli* (pMD4) grown in LB medium without metal supplementation, contained 0.5 iron atom per 52.4 kDa monomeric polypeptide subunit. Subsequent studies, using increased protein concentrations during protein purification procedures, resulted in protein with 1.18 ± 0.03 iron atoms per subunit. ICP analysis indicated that there was less than 0.08 manganese, copper, chromium, nickel, cadmium, cobalt, or zinc atom per protein subunit. Treatment of the enzyme with 1,10-phenanthroline reduced the iron content to 0.07−0.14 atom per monomer and produced an enzyme with negligible activity (3−8%). The apoenzyme preparations used for Co(II) reconstitution routinely contained 0.12 ± 0.02 iron atom per subunit.

Reconstitution of several different apoenzyme preparations with Co(II) resulted in AtzA containing cobalt at a level of 0.5−0.9 atom per subunit. The Co(II) content of Co(II)−AtzA paralleled activity increases when copper was absent (Table 2, Co(II)−AtzA preparations 1 and 3). Iron levels in the Co(II)−AtzA did not differ significantly from those of apoenzyme preparations. With the presence of both cobalt and iron, the reconstituted metal-to-subunit ratio ranged from 0.5 to 1.0. Co(II)−AtzA (212 μM) was treated with $CuCl_2$ (550 μM), passed through a Sephadex G-25 column to separate the protein from unbound metal, and analyzed for metal content. The enzyme had 2.5 copper atoms bound per subunit, but 0.5 cobalt and 0.1 iron atoms were still bound per subunit. Thus, cobalt and the residual iron remained bound to the enzyme after copper binding. The inhibitory effects of copper are also observed in Co(II)−AtzA preparation 2 (Table 2). Thus, the presence of copper in preparation 2 is most likely the reason for its observed lower activity compared to those of the other preparations.

Chelator Effects and Apoenzyme Preparation. AtzA treated with 1,10-phenanthroline had an absorbance maximum at 510 nm. This wavelength corresponds to a metal−1,10-phenanthroline complex (*31*−*34*), which can be removed from the enzyme by dialysis. Enzymatic activity decreased over a 90 min period with a corresponding increase in

Table 2: Metal Content of AtzA Preparations[a]

enzyme	activity (units/mg)	concn (μM) AtzA subunit	Fe	Co	Cu	metal:subunit ratio Fe	Co	Fe + Co
native	4.1	76.6	37.5	nd	nd	0.5	nd	0.5
1,10-phenanthroline, metal stripped	<0.01	7.6	0.5	nd	nd	0.07	nd	0.07
Co(II)−AtzA, prep 1	8.0	24.9	2.8	12.2	nd	0.1	0.5	0.6
Co(II)−AtzA, prep 2	5.0	12.5	1.8	9.1	2.5	0.1	0.7	0.8
Co(II)−AtzA, prep 3	12.0	27	3.2	24.2	nd	0.1	0.9	1.0
Cu(II)-treated Co(II)−AtzA, prep 1	0.2	11.6	1.4	5.8	29.0	0.1	0.5	0.6

[a] nd = not detected, less than 0.20 μM Co or 0.41 μM Cu.

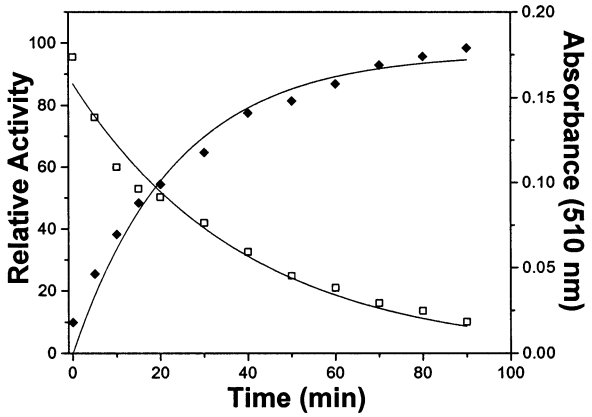

FIGURE 2: Inactivation of AtzA by 1,10-phenanthroline. AtzA (32.6 μM) was incubated with 0.5 mM 1,10-phenanthroline in 25 mM MOPS−NaOH, pH 6.9, 10 mM KCl at 23 °C. $A_{510\,nm}$ from the 1,10-phenanthroline−metal complex was monitored (◆). Aliquots were removed at the indicated times and assayed for activity. Activities were expressed as a percentage of the initial activity (4.5 (μmol/min)/mg) (□). The curves represent a first-order fit to the data.

Table 3: Activation of AtzA Apoenzyme by Metals[a]

addition	% relative native activity	addition	% relative native activity
none	4 ± 1	0.2 mM $NiCl_2$	4 ± 1
0.2 mM $MnSO_4$	23 ± 6	0.2 mM $CuCl_2$	1 ± 0
1 mM $MgCl_2$	3 ± 1	0.2 mM $CoCl_2$	241 ± 47
0.5 mM $CaCl_2$	3 ± 1	0.2 mM $FeSO_4$, 0.5 mM cysteine, 1.5 mM DTT	105 ± 27
0.2 mM $FeCl_3$	4 ± 1	0.5 mM cysteine, 1.5 mM DTT	3

[a] Activities were determined for two different enzyme preparations and expressed as a percentage of the native enzyme activity (4.4 and 3.0 (μmol/min)/mg). Averages of the two preparations are displayed in the table.

absorbance at 510 nm (Figure 2). A first-order fit of these data produced rate constants of 0.3 and 0.4 min^{-1}, respectively. Subsequent chelation experiments routinely reduced AtzA activity to less than 3% of the holoenzyme activity. AtzA, incubated at 23 °C for 90 min in the absence of 1,10-phenanthroline, retained greater than 95% activity. In addition, AtzA incubated with a 25 μM concentration of the chelator oxalic acid had no detectable chlorohydrolase activity (data not shown).

Reconstitution of Apoenzyme with Metals. Reconstitution of enzyme activity was tested by incubating apoenzyme with various metals (Table 3). The metals were preincubated with apoenzyme for 15 min to 12 h. No increase in activity was observed with longer incubation times. The presence of 100 mM sodium bicarbonate in reconstitution experiments did not affect enzymatic activity or reconstitution times. Incubation with Co(II), Fe(II), or Mn(II) significantly activated the enzyme. However, Fe(III), Mg(II), Ca(II), and Ni(II) did not reconstitute activity, and Cu(II) caused a decrease in the small amount of residual activity present in the apoenzyme.

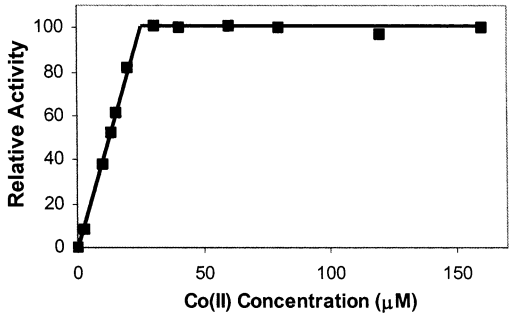

FIGURE 3: Activation of AtzA apoenzyme by Co(II). AtzA apoenzyme (27 μM) was incubated with the indicated concentrations of $CoCl_2$ in buffer A for 12 h at 23 °C and assayed for activity. Activities were expressed as a percentage of the maximum activity (12.0 (μmol/min)/mg).

Because DTT and cysteine, used in this study to maintain the iron in an Fe(II) oxidation state, showed inhibitory effects on AtzA (Table 1), Co(II) or Fe(II) was also added to a different apoenzyme preparation without thiol reagents and under anaerobic conditions. When reconstituted with Fe(II), the activity was 180 ± 73% of the original native enzyme. The Co(II)-reconstituted apoenzyme had an activity of 201 ± 53% of the native enzyme. This is significantly higher than that of the native enzyme, though not significantly different from that of the Fe(II)-reconstituted enzyme. These results show that both Fe(II) and Co(II) can reconstitute apoAtzA to activities equal to or greater than that seen with the native enzyme.

Co(II) Reconstitution Stoichiometry. The dependence of AtzA activity on Co(II) concentration was assayed in reconstitution experiments (Figure 3). ApoAtzA (27 μM) was incubated with varying concentrations of Co(II). The activity of the enzyme increased linearly as a function of increasing Co(II) concentrations at substoichiometric concentrations. Maximum activity was at 24 μM Co(II), corresponding to 0.9 cobalt atom per polypeptide monomer.

Zn(II) Effects on AtzA. Zn(II) added to holoenzyme in large excess inhibited enzyme activity (Table 1). However, activation was observed when apoAtzA was incubated with Zn(II) at concentrations up to a 1:1 stoichiometry with respect to the polypeptide subunit (Figure 4). This result suggested that Zn(II) can coordinate at the same metal binding site as

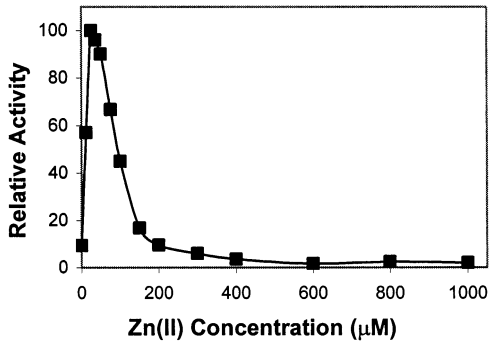

FIGURE 4: Effect of Zn(II) on the activity of apoAtzA. Apoenzyme (27 μM) was incubated with the indicated concentrations of $ZnSO_4$ in buffer A at 23 °C for 30 min before assaying for activity. Activities were expressed as a percentage of the maximum activity (1.5 (μmol/min)/mg).

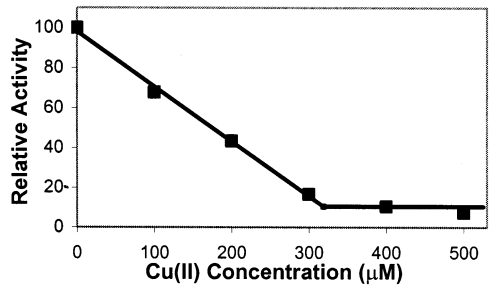

FIGURE 5: Inhibition of Co(II)−AtzA by titrating Cu(II). Co(II)−AtzA (212 μM) was incubated with the indicated $CuCl_2$ concentrations in buffer A for 30 min at 23 °C prior to assaying for activity. Activities were expressed as a percentage of the initial activity (4.6 (μmol/min)/mg).

Co(II) to reconstitute activity. Activation peaked at 25 μM $ZnSO_4$ with an apoenzyme concentration of 27 μM. This corresponds to 0.9 zinc atom per polypeptide. Inhibitory effects became apparent at higher concentrations of Zn(II) (Figure 4). These data suggest that there is a relatively high affinity binding site for one zinc atom per subunit at the active site, and at least one lower affinity binding site for zinc that, when occupied, inhibits activity.

Cu(II) Inhibition of AtzA. Addition of 550 μM Cu(II) to 212 μM Co(II)−AtzA was shown to bind at a 2.5 metal to subunit ratio (Table 2); therefore, Co(II)−AtzA effectively bound all of the Cu(II) in solution. This finding suggests that either Cu(II) binds irreversibly or the off-rate for Cu(II) binding is extremely slow, with nearly all Cu(II) remaining bound even after passage through a Sephadex G-25 column in metal-free buffer. Strikingly, Cu(II) did not displace cobalt or iron from the enzyme (Table 2). Furthermore, Co(II)−AtzA was inhibited by Cu(II) (Figure 5). Assuming that inhibition of AtzA activity reflects Cu(II) binding, the data were fit to a number of binding curves. The curve for irreversible binding, with a correlation coefficient of 0.9965, is shown in Figure 5. From this fit, maximum inhibition of Co(II)−AtzA was achieved at approximately 320 μM Cu(II), a Cu(II) to subunit stoichiometry of 1.7. At maximal inhibition, approximately 10% activity remained. Increasing the stoichiometric ratio to 2.5 did not significantly change this residual activity. These analyses of Co(II)−AtzA suggest that Cu(II) binds, irreversibly and/or with slow dissociation, at a minimum of two sites, none of which are the catalytic metal site.

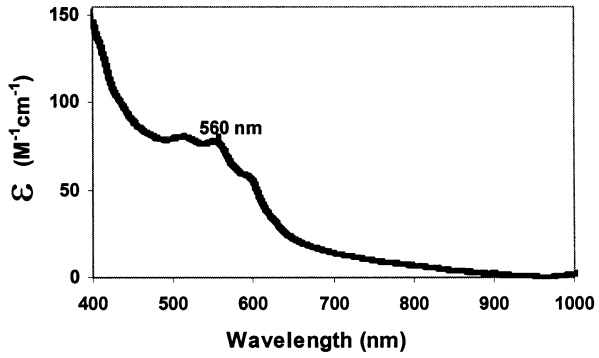

FIGURE 6: Representative visible absorbance difference spectrum of Co(II)−AtzA minus apoAtzA (438 μM). Extinction coefficients were determined on the basis of Co(II) concentrations and assuming a baseline zero absorbance at 970 nm.

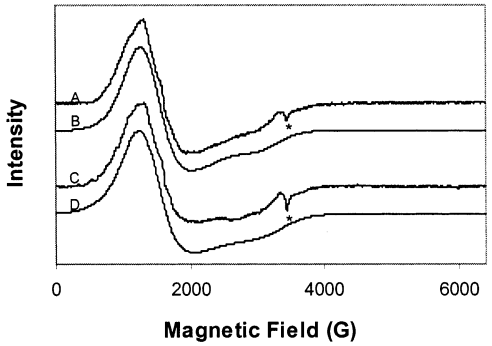

FIGURE 7: EPR spectra of Co(II)−AtzA in the presence or absence of the substrate analogue aminoatrazine: (A) spectrum for Co(II)−AtzA (438 μM) without aminoatrazine, (B) simulation of (A) with g_{eff} values of 4.92, 4.13, and 2.25, (C) spectrum for Co(II)−AtzA with aminoatrazine, and (D) simulation of (C) with g_{eff} values of 4.91, 4.10, and 2.24. A small amount of extraneous Cu(II) was present in all samples and buffers and is seen as a negative peak at around $g = 2$ (*). EPR conditions: 10 K, microwave power 781 μW, modulation amplitude 10 G, microwave frequency 9.609 GHz for (A) and 9.600 GHz for (C).

Visible Spectra of AtzA. A visible difference spectrum of Co(II)−AtzA minus apoAtzA, representative of two different samples, is shown in Figure 6. The extinction coefficient was 73 ± 22 M^{-1} cm^{-1} at 560 nm.

EPR Spectroscopy of AtzA. EPR spectra of Co(II)−AtzA were obtained and simulated (Figure 7A,B) to obtain $g_{eff(x,y,z)}$ values of 4.92 (4.92), 4.13 (4.14), and 2.25 (2.25), respectively. These values correspond to a g_{real} of 2.270 and an E/D of 0.058 in an $M_s = |\pm^1/_2\rangle$ ground-state transition. Addition of the substrate analogue aminoatrazine produced only a slight broadening of the EPR spectrum (Figure 7C,D). The $g_{eff(x,y,z)}$ values of the spectra were 4.91 (4.91), 4.10 (4.10), and 2.24 (2.24), corresponding to an $M_s = |\pm^1/_2\rangle$ ground-state transition with g_{real} and E/D values of 2.259 and 0.060, respectively.

Power saturation studies were performed to determine the coordination number of the metal center. The normalized intensity was measured as a function of power for six different temperatures (Figure 8, inset). For each biphasic curve, the point at which the asymptotic limits intersect is the power at which the saturation factor is 0.5, known as $P_{1/2}$. Fitting a plot of the temperature dependence of $P_{1/2}$ versus the reciprocal of temperature (Figure 8) provided an estimate that the zero-field splitting parameter (Δ or $2|D|$)

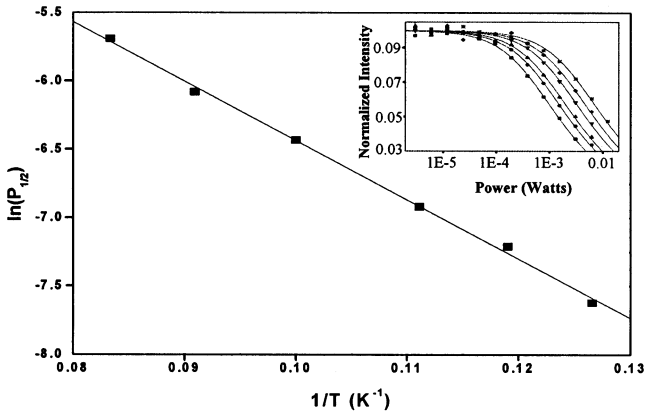

FIGURE 8: Power saturation studies for Co(II)−AtzA (438 μM). The inset displays the power saturation curves of normalized signal intensity versus power at various temperatures: (from left to right) (■) 7.9 K, (●) 8.4 K, (▲) 9 K, (▼) 10 K, (◆) 11 K, and (*) 12 K. The $P_{1/2}$ values were calculated from the fitted curves and plotted as a function of reciprocal temperature in the larger figure.

was 30 cm^{-1} for Co(II)−AtzA. The estimate is valid only if the spin−lattice relaxation is predominately due to the Orbach process. The three conditions required for the curve to be in the Orbach domain were met. First, at high power, the *b* values did not vary over the temperature range studied. Second, the unsaturated linewidth was similarly invariant with temperature. Third, the lineshape did not change with saturating microwave fields. Therefore, the estimate of the zero-field splitting parameter presented here is considered valid for Co(II)−AtzA.

DISCUSSION

AtzA has been found only in bacteria that metabolize the herbicide atrazine (*35*) and catalyzes the initiating reaction in the biodegradation of this widely used herbicide. AtzA hydrolytically dechlorinates atrazine to yield hydroxyatrazine. In a previous study, metals were not implicated in the catalysis of atrazine by AtzA (*13*). Here, however, we provide evidence from sequence analyses and experiments that AtzA is a member of the amidohydrolase protein superfamily and a metalloenzyme.

The amidohydrolase superfamily is characterized by a conserved $(\beta\alpha)_8$ barrel structure. Superfamily members generally have conserved metal binding ligands and a common hydrolytic mechanism in which one or two metals are responsible for activating water for nucleophilic attack on the substrate. This superfamily is most heavily represented by enzymes catalyzing amide bond hydrolysis and the hydrolytic displacement of amino groups from heterocyclic ring substrates. The latter function includes the enzymes adenosine deaminase and cytosine deaminase, which are involved in purine/pyrimidine metabolism.

Though dechlorination is not known to be the major activity of any other member of the amidohydrolase superfamily, some superfamily members have been shown to catalyze hydrolytic dechlorination reactions. Adenosine deaminase is capable of catalyzing hydrolytic displacement of chloride from chloropurine substrate analogues (*36*−*38*). However, the rate of dechlorination was 10-fold lower than deamination activity, suggesting that the dechlorination reaction is likely fortuitous. The *s*-triazine hydrolase enzyme TrzA has also been shown to catalyze both deamination and dechlorination reactions (*24*). However, the substrates that are deaminated have structural features different from those of the substrates that are dechlorinated. TrzA catalyzes the deamination of *s*-triazine substrates that do not contain *N*-alkyl side chains and the dechlorination of *s*-triazines with a single *N*-alkyl side chain. Since atrazine and its amino analogue aminoatrazine contain two *N*-alkyl side chains, they are not substrates for TrzA. As with adenosine deaminase, the deamination reactions of TrzA proceed 100 times faster then the dechlorination reactions. Though other superfamily enzymes exhibit fortuitous dechlorination reactions, AtzA is unique in that it only catalyzes dechlorination reactions, without the ability to catalyze deamination reactions of substrate analogues (*39*).

Like other members of the amidohydrolase superfamily, a metal has been implicated in AtzA activity. In this study, we show that maximal AtzA activity was obtained with Co(II) or Zn(II) at a 1:1 metal to subunit stoichiometry. Though initial experiments showed a metal to subunit stoichiometry of the native enzyme to be 0.5 (Table 2), later experiments with different enzyme preparations contained 1.18 ± 0.03 iron atoms bound per subunit. The properties of AtzA established in this study most closely resemble cytosine deaminase from *E. coli*. The crystal structure of cytosine deaminase revealed a mononuclear iron metal at the active site (*21*). Activity assays also showed that cytosine deaminase was activated by Fe(II), Co(II), and Mn(II) (*40*), a property found here to be shared by AtzA.

Cytosine deaminase and AtzA are the only known members of the amidohydrolase superfamily that contain Fe(II) as the catalytic metal. It is additionally noteworthy that the presence of Fe(II) in a hydrolytic enzyme is not common. The first recognized Fe(II)-dependent amidase, peptide deformylase, was identified as recently as 1997 (*41*). This enzyme catalyzes the removal of the N-terminal formyl group from ribosome-synthesized polypeptides in bacteria. However, the activity of peptide deformylase is extremely unstable, with an activity half-life of 2 min in assays done aerobically at room temperature (*42*). Crystallization of this enzyme revealed a structure, consisting of three α-helices, three β-sheet regions, and a 3−10 helix, that is quite different from the structures of amidohydrolase superfamily enzymes. The peptide deformylase metal is tetrahedrally coordinated by two histidines, a cysteine, and a water molecule (*41*, *43*). On the basis of the conservation of an HEXXH motif that contains the two metal histidine ligands, peptide deformylase was identified as belonging to a family of otherwise mostly zinc metallopeptidases that includes thermolysin (*43*).

In contrast, the metal center in natively isolated AtzA was shown to be stable for 24 h under aerobic conditions at room temperature with less than a 3% loss in activity. Cytosine deaminase was also shown to be active when reconstituted with Fe(II), without rapid loss of activity (*40*), and was crystallized with Fe(II) (*21*). Therefore, the $(\beta\alpha)_8$ barrel structure of the amidohydrolase superfamily likely stabilizes the Fe(II) and prevents rapid oxidation.

The data obtained from Zn(II) and Cu(II) inhibition of AtzA activity suggest that their inhibitory effects are not caused by replacing the catalytic metal at the active site. Therefore, other metal binding sites most likely mediate the inhibitory effects of these metals. Like AtzA, cytosine deaminase was shown to obtain maximal activity at a nearly

1:1 Zn(II) to subunit ratio, with excess Zn(II) causing inhibition (*44*). Inhibition of enzymatic activity with Cu(II) has been reported for many amidohydrolase superfamily members, including cytosine deaminase and adenosine deaminase (*40*, *45*). The fact that Cu(II) was shown here not to alter the binding stoichiometry of active site metals suggests that Cu(II) inhibits AtzA by binding to the enzyme at location(s) other than where the active site metal is found, implicating secondary metal binding sites that have inhibitory effects on AtzA activity.

In a previous study, we identified AtzC as containing a simplified version of the N-terminal dihydroorotase signature pattern identified in Prosite entry PS00482 (*17*), namely, DXHXH. AtzA was also identified as a putative member of the amidohydrolase superfamily on the basis of conservation of the HXH metal binding motif. Since both mononuclear and dinuclear members of the amidohydrolase superfamily contain the same basic set of metal binding ligands, sequence identity around the first two metal ligands is not sufficient to assign it to either a mononuclear or dinuclear metal binding phenotype. The experiments presented here were essential for determining the number of metals at the AtzA activite site. It should be noted that the C-terminal dihydroorotase signature pattern identified in Prosite, around the aspartate metal binding ligand, is not present in any of the triazine-degrading enzymes AtzA, AtzB, and AtzC.

Further evidence that AtzA has a mononuclear metal center originates from analyzing the biochemical properties of dinuclear members of the amidohydrolase superfamily for which crystal structures are available, including urease, phosphotriesterase, and dihydroorotase (*19*, *46*, *47*). Urease contains two Ni(II) ions at the active site, while the other two enzymes have Zn(II). Most dinuclear enzymes are known to contain a carbamylated lysine residue that acts as a bridging ligand between the metals of the dinuclear cluster. Effective apoenzyme reconstitution requires that the lysine be carbamylated prior to metal addition. Previous studies have shown that the presence of the metal prior to carbamylation of the lysine actually prevents subsequent lysine carbamylation (*48*, *49*). For AtzA, the observed metal stoichiometries, coupled with results showing that metal reconstitution of AtzA activity does not require carbamylation, are consistent with the view that AtzA most likely contains a mononuclear metal center.

Though the catalytic metals in various members of the superfamily include a range of elements, the coordination and function of the metals are conserved. Comparison of the crystal structures available for dinuclear and mononuclear members of the superfamily reveals that the active sites of both types are nearly superimposable (*19*). Most dinuclear members of the superfamily ligate their metals by using a His-X-His site, two additional histidines, an aspartate, a bridging carbamylated lysine, and a bridging water molecule, resulting in one metal being four-coordinate and the second metal being five-coordinate. A key difference between the mononuclear and most dinuclear active sites is the absence of the carbamylated lysine and the fourth histidine as metal ligands in the mononuclear enzymes. Although this fourth histidine is conserved in the mononuclear members, it is involved in hydrogen bonding to the water ligand instead of ligating a metal. The resulting metal is therefore a five-coordinate species.

Since Fe(II) is EPR silent and the holoenzyme had virtually no EPR signal, Co(II)−AtzA was used in our spectroscopic studies. The electronic spectrum yielded an extinction coefficient of 73 ± 22 M^{-1} cm^{-1} at 560 nm. General guidelines in the literature for coordination of Co(II) indicate that extinction coefficients for peaks between 400 and 900 nm are usually below 50 for six-coordination, between 50 and 300 for five-coordination, and greater than 300 for four-coordination (*50*, *51*). These values suggest that the cobalt center in AtzA is five- or six-coordinate.

The EPR spectra of Co(II)−AtzA were reasonably well-simulated as a single, paramagnetic metal center. Further, power saturation studies were used to estimate the zero-field splitting parameter of the Co(II)−AtzA to be 30 cm^{-1}. This parameter has been shown to be related to the coordination number of Co(II). Values greater than 46 cm^{-1} are generally for six-coordination, values between 30 and 46 cm^{-1} are for five-coordination, and values less than 30 cm^{-1} are for four-coordination (*27*, *52*). On the basis of the zero-field splitting value, AtzA could be either four- or five-coordinate. Studies in the literature have also shown that it is difficult to delineate between four- and five-coordination by this method (*53*). Taken together, results from visible and EPR spectroscopy implicate a five-coordinate metal center in AtzA. A single, diamagnetic, five-coordinate metal center is consistent with the evidence that AtzA is a mononuclear member of the amidohydrolase protein superfamily.

In summary, the evidence presented here suggests that AtzA has a mononuclear five-coordinate metal center that natively binds Fe(II) at the active site. All known *s*-triazine catabolic enzymes that remove groups from an *s*-triazine ring, including AtzB, AtzC, TrzA, TriA, TrzC, and TrzN, are evolutionarily related to AtzA. Therefore, they are also members of the amidohydrolase superfamily and expected to potentially bind catalytically essential metals. The present study elucidates some essential properties of AtzA and provides information about the larger group of enzymes involved in the bacterial metabolism of industrially relevant *s*-triazine compounds.

ACKNOWLEDGMENT

The authors thank Professor John Lipscomb for making available the EPR spectrometer, Matt Neibergall for assistance with the EPR spectrometer, and Codrina Popeseu for helpful discussions.

REFERENCES

1. Copley, S. D. (2000) *Trends Biochem. Sci. 25*, 261−5.
2. Lee, M. D., Odom, J. M., and Buchanan, R. J. J. (1998) *Annu. Rev. Microbiol. 52*, 423−52.
3. van der Meer, J. R. (1997) *Antonie Van Leeuwenhoek 71*, 159−78.
4. Abramowicz, D. A. (1995) *Environ. Health Perspect. 103*, 97−9.
5. Leisinger, T., and Braus-Stromeyer, S. A. (1995) *Environ. Health Perspect. 103*.
6. Chaudhry, G. R., and Chapalamadugu, S. (1991) *Microbiol. Rev. 55*, 59−79.
7. Wackett, L. P. (1991) *Appl. Enzyme Biotechnol.* 191−200.
8. Wackett, L. P. (1994) *Curr. Opin. Biotechnol. 5*, 260−265.
9. Radosevich, M., Traina, S. J., Hao, Y., and Tuovinen, O. H. (1995) *Appl. Environ. Microbiol. 61*, 297−302.
10. Mandelbaum, R. T., Wackett, L. P., and Allan, D. L. (1993) *Appl. Environ. Microbiol. 59*, 1695−1701.

11. Moscinski, J. K., Jayachandran, K., and Moorman, T. B. (1996) *96th General Meeting of the American Society for Microbiology*, p 458, American Society for Microbiology, New Orleans, LA.
12. Mandelbaum, R. T., Allan, D. L., and Wackett, L. P. (1995) *Appl. Environ. Microbiol. 61*, 1451−1457.
13. de Souza, M. L., Sadowsky, M. J., and Wackett, L. P. (1996) *J. Bacteriol. 178*, 4894−4900.
14. Verschueren, K. H. G., Franken, S. M., Rozeboom, H. J., Kalk, K. H., and Dijkstra, B. W. (1993) *J. Mol. Biol. 232*, 856−872.
15. Yang, G., Liu, R. Q., Taylor, K. L., Xiang, H., Price, J., and Dunaway-Mariano, D. (1996) *Biochemistry 35*, 10879−10885.
16. Ridder, I. S., Rozeboom, H. J., Kalk, K. H., and Dijkstra, B. W. (1999) *J. Biol. Chem. 274*, 30675−8.
17. Sadowsky, M. J., Tong, Z., de Souza, M. L., and Wackett, L. P. (1998) *J. Bacteriol. 180*, 152−158.
18. Holm, L., and Sander, C. (1997) *Proteins 28*, 72−82.
19. Jabri, E., Carr, M. B., Hausinger, R. P., and Karplus, P. A. (1995) *Science 268*, 998−1003.
20. Wilson, D. K., and Quiocho, F. A. (1993) *Biochemistry 32*, 1689−94.
21. Ireton, G. C., McDermott, G., Black, M. E., and Stoddard, B. L. (2002) *J. Mol. Biol. 315*, 687−697.
22. de Souza, M. L., Wackett, L. P., Boundy-Mills, K. L., Mandelbaum, R. T., and Sadowsky, M. J. (1995) *Appl. Environ. Microbiol. 61*, 3373−3378.
23. Sambrook, J., Fritsch, E. F., and Maniatis, T. (1989) *Molecular Cloning: A Laboratory Manual*, 2nd ed., Cold Spring Harbor Press, Cold Spring Harbor, NY.
24. Mulbry, W. W. (1994) *Appl. Environ. Microbiol. 60*, 613−618.
25. Bennett, B., and Holz, R. C. (1997) *J. Am. Chem. Soc. 119*, 1923−33.
26. Bennett, B., and Holz, R. C. (1997) *Biochemistry 36*, 9837−46.
27. Yim, M. B., Kuo, L. C., and Makinen, M. W. (1982) *J. Magn. Reson. 46*, 247−256.
28. Makinen, M. W., and Yim, M. B. (1981) *Proc. Natl. Acad. Sci. U.S.A. 78*, 6221−5.
29. Makinen, M. W., Kuo, L. C., Yim, M. B., Wells, G. B., Fukuyama, J. M., and Kim, J. E. (1985) *J. Am. Chem. Soc. 107*, 5245−55.
30. Sahlin, M., Graeslund, A., and Ehrenberg, A. (1986) *J. Magn. Reson. 67*, 135−7.
31. Wagner, F. W. (1988) in *Methods in enzymology* (Riordan, J. F., and Vallee, B. L., Eds.) pp 21−32, Academic Press, Inc., San Diego.
32. Auld, D. S. (1988) in *Methods in Enzymology* (Riordan, J. F., and Vallee, B. L., Eds.) pp 110−114, Academic Press Inc., San Diego.
33. Santos, N. C., Castilho, R. F., Meinicke, A. R., and Hermes-Lima, M. (2001) *Eur. J. Pharmacol. 428*, 37−44.
34. Thomas, L. C., and Chamberlin, G. J. (1980) *Colorimetric chemical analytical methods*, 9th ed., John Wiley and Sons Ltd., New York.
35. de Souza, M. L., Seffernick, J., Martinez, B., Sadowsky, S. J., and Wackett, L. P. (1998) *J. Bacteriol. 180*, 1951−1954.
36. Baer, H. P., Drummond, G. I., and Duncan, E. L. (1966) *Mol. Pharmacol. 2*, 67−76.
37. Bar, H. P., and Drummond, G. I. (1966) *Biochem. Biophys. Res. Commun. 24*, 584−587.
38. Cory, J. G., and Sunhadolnik, R. J. (1965) *Biochemistry 4*, 1733−1735.
39. Seffernick, J. L., Johnson, G., Sadowsky, M. J., and Wackett, L. P. (2000) *Appl. Environ. Microbiol. 66*, 4247−52.
40. Porter, D. J. T., and Austin, E. A. (1993) *J. Biol. Chem. 268*, 24005−24011.
41. Rajagopalan, P. T. R., Yu, X. C., and Pei, D. (1997) *J. Am. Chem. Soc. 119*, 12418−9.
42. Rajagopalan, P. T. R., Datta, A., and Pei, D. (1997) *Biochemistry 36*, 13910−8.
43. Chan, M. K., Gong, W., Rajagopalan, P. T. R., Hao, B., Tsai, C. M., and Pei, D. (1997) *Biochemistry 36*, 13904−9.
44. Porter, D. J. (2000) *Biochim. Biophys. Acta 1476*, 239−52.
45. Cooper, B. F., Sideraki, V., Wilson, D. K., Dominguez, D. Y., Clark, S. W., Quiocho, F. A., and Rudolph, F. B. (1997) *Protein Sci. 6*, 1031−1037.
46. Benning, M. M., Kuo, J. M., Raushel, F. M., and Holden, H. M. (1994) *Biochemistry 33*, 15001−15007.
47. Thoden, J. B., Phillips, G. N., Jr., Neal, T. M., Raushel, F. M., and Holden, H. M. (2001) *Biochemistry 40*, 6989−97.
48. Yamaguchi, K., Cosper, N. J., Stalhandske, C., Scott, R. A., Pearson, M. A., Karplus, P. A., and Hausinger, R. P. (1999) *J. Biol. Inorg. Chem. 4*, 468−77.
49. Shim, H., and Raushel, F. M. (2000) *Biochemistry 39*, 7357−64.
50. Bertini, I., and Luchinat, C. (1984) *Adv. Inorg. Biochem. 6*, 71−111.
51. Banci, L., Bencini, A., Benelli, C., Gatteschi, D., and Zanchini, C. (1982) *Struct. Bonding 52*, 37.
52. Makinen, M. W., Kuo, L. C., Dymowski, J. J., and Jaffer, S. (1979) *J. Biol. Chem. 254*, 356−366.
53. Larrabee, J. A., Alessi, C. M., Asiedu, E. T., Cook, J. O., Hoerning, K. R., Klingler, L. J., Okin, G. S., Santee, S. G., and Volkert, T. L. (1997) *J. Am. Chem. Soc. 119*, 4182−96.

BI020415S